Breakup of spiral and concentric ringed spherulites in polymer crystallization

Haijun Xu, Hao-Wen Chiu, Yoshifumi Okabe, and Thein Kyu
Department of Polymer Engineering, University of Akron, Akron, Ohio 44325, USA
(Received 28 February 2006; published 5 July 2006)

Recently, the breakup of spiral and concentric ringed spherulites has been observed experimentally in isothermal crystallization of poly(vinylidene fluoride) in its blends with ethylene vinyl acetate copolymer. To elucidate the phenomenon of spiral breakup in polymer spherulites, a theoretical simulation has been undertaken in the framework of the phase field model of solidification based on time-dependent Ginzburg-Landau equations (TDGL model C) pertaining to the conserved concentration and nonconserved phase field order parameters. The concentration order parameter was described in terms of the Landau-type potential, while the crystal order parameter was expressed in terms of an asymmetric double-well potential to account for the nonequilibrium nature (i.e., metastability) of polymer crystallization. After inserting these potentials into the TDGL model C, the resulting coupled time-evolution equations show the emergence of the target and spiral patterns that undergo fragmentation at a very shallow supercooling. It is concluded that the depth of supercooling is the major contributor to the formation of the spirals and subsequent breakup of the spiral arms.

DOI: 10.1103/PhysRevE.74.011801 PACS number(s): 61.41.+e, 64.75.+g, 64.60.Cn

INTRODUCTION

The target (concentric rings) and spiral growth in polymer spherulites has gained renewed interest in polymer crystallization [1,2] due to its similarity to the pattern forming aspects of nonlinear dynamics in chemical reactions and excitable media [3,4]. In previous papers [1,2], the emergence of the spiral spherulite has been shown experimentally [1] as well as theoretically [2] in blends of poly(vinylidene fluoride) (PVDF) and polyvinyl acetate (PVAc). The former is the crystalline polymer while the latter is the amorphous material. In the context of the phase field model that describes directional solidification [4–6], it was demonstrated that the phase field model based on the time-dependent Ginzburg-Landau equations [7,8] [TDGL model C, i.e., the combination of model A and model B, alternatively known as Cahn-Hilliard equation [9] (TDGL model B) and Allen-Cahn equation [10] (TDGL model A)] [11], having appropriate asymmetric double-well free energy and coupling coefficients, is capable of predicting the spatiotemporal evolution of spiral spherulites in crystalline polymer blends [2,12]. Although the growth patterns of spiral spherulites in polymer crystallization are strikingly similar to the pattern formation in chemical reactions and biological organization [3], the mechanism is drastically different in that the core of the spherulite [1,2] (crystal nucleus) is not pulsating as opposed to those in the excitable media [3].

As a continuation effort, we have undertaken the crystallization study in miscible blends of PVDF and ethylene-vinyl acetate copolymer (EVA-80) having vinyl acetate content of 80 mol %. In isothermal crystallization of poly(vinylidene fluoride) in its blends, the breakup of spiral and concentric ringed spherulites has been observed experimentally. To describe the phenomenon of spiral breakup in polymer spherulites, a theoretical model has been proposed in the framework of the phase field model for solidification based on the TDGL model C by coupling conserved concentration and nonconserved crystal order parameters. The concentration order parameter was described in the context of the Landau-type potential, whereas the crystal order parameter was expressed in terms of an asymmetric double-well potential to ensure its applicability to the first-order phase transition involving latent heat of crystallization. Of particular importance is that the simulation captures the emergence of the target and spiral patterns which undergo fragmentation at a very shallow supercooling. The effect of supercooling on the pattern forming aspects of polymer spherulites is discussed.

THEORETICAL SCHEME

In atomic crystals, crystallization phenomena have been generally analyzed in the context of the classical macroscopic models of phase transitions. The governing equations treat thermodynamic variables such as temperature and concentration of the individual phases independently with a discrete interface of zero thickness [13]. The proposed phase field model [5,6], based on incorporation of the asymmetric free energy functional for crystal phase transitions into the TDGL model C, describes the crystal-melt boundary as smooth interface. The purpose of present paper is to examine whether or not (i) the phase field model is capable of generating the nonpulsating target/spiral pattern and (ii) the instability of the emerging spiral spherulites, driven by the interplay between polymer demixing (or miscibility) and crystallization, plays any role in the breakup of the spiral arms.

A theoretical model has been developed in the framework of the phase field model based on the TDGL model C equations for the conserved composition order parameter for the blends and nonconserved phase order parameters pertaining to the free energy functional of crystal ordering (crystallization), *viz.*,

$$F(\phi,\psi)=\int\left[f_{conc}(\phi)+f_{cryst}(\psi)+f_{coupling}(\phi,\psi)+\frac{1}{2}\kappa_{\phi}(\nabla\phi)^2+\frac{1}{2}\kappa_{\psi}(\nabla\psi)^2\right]d\Omega, \quad (1)$$

where

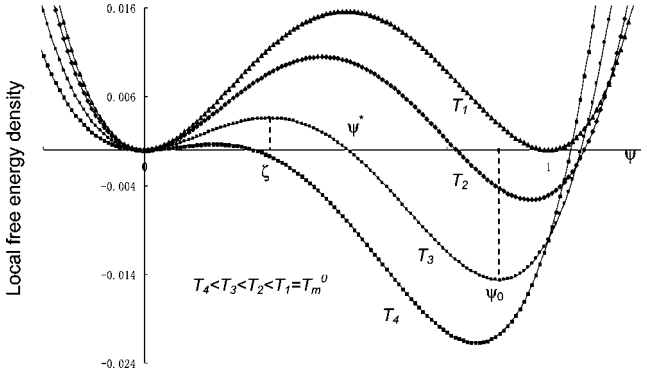

FIG. 1. Variation of the local free energy density as a function of crystal order parameter ψ for various temperatures showing different nucleation barrier heights and locations, ζ. The crystal state $\psi=\psi_0$ varies with the crystallization temperature indicating the imperfection of polymer crystals.

$$f_{conc}(\phi) = \frac{r}{2}\phi^2 + \frac{u}{4}\phi^4, \tag{2}$$

$$f_{cryst}(\psi) = W_\psi\left[\frac{\zeta(T)\psi_0}{2}\psi^2 - \frac{\zeta(T)+\psi_0}{3}\psi^3 + \frac{\psi^4}{4}\right], \tag{3}$$

$$f_{coupling}(\phi,\psi) = -(\alpha_1\psi\phi + \alpha_2\psi^2\phi + \alpha_3\psi\phi^2), \tag{4}$$

where κ_ϕ and κ_ψ are the coefficients of gradient of concentration and the crystal order parameters. Equation (2) is a typical Landau-type free energy in which the sign of r determines whether the potential is a single-well ($r>0$) representing miscible blends or a symmetric double-well ($r<0$) representing phase separated systems in the limit of $-0.5\leqslant\phi\leqslant 0.5$. Alternatively, one can use the Flory-Huggins-type free energy that exhibits a single well for a miscible system, but a double well for a two-phase system in the limit of $0\leqslant\phi\leqslant 1$. The third-order expansion coefficient should be taken into consideration if the potential of the concentration field were an asymmetric double-well, but for simplicity, it is set to zero here.

Equation (3) represents the free energy density pertaining to the crystal order parameter which may be defined as the linear crystallinity, $\psi=\ell/\ell^o$, where ℓ and ℓ^o are the lamellar thickness and the thickness of the perfect crystal. In view of the imperfect nature of polymer crystals and the metastability of the crystallization, the order parameter at the solidification potential is defined to be temperature dependent such that $\psi_0=T_m/T_m^0$, where T_m^0 is equilibrium melting temperature, where T_m is the obtained melting temperature at a given crystallization temperature T. Except at equilibrium, this order parameter ψ_0 is always less than unity, which implies the imperfect nature of polymer crystallinity. W_ψ is the dimensionless coefficient and ζ is the location of the nucleation barrier peak on the ψ axis of the asymmetric double-well potential that accounts for the metastability and latent heat of crystallization (Fig. 1).

Equation (4) represents the coupling term for concentration and crystal ordering in which α_1, α_2, and α_3 are the coupling strengths. Higher order coupling terms of the two order parameters (i.e., ϕ and ψ) as well as the coupling between their gradients are neglected in Eq. (3), as the two gradient terms in Eq. (1) are sufficient to describe the present system. Regarding the temporal evolution of these two order parameters, the total free energy may be substituted in the TDGL model C that basically involves two nonlinear diffusion equations in which a conserved compositional order parameter (ϕ) is coupled with a nonconserved phase field parameter, hereafter called the crystal order parameter (ψ), *viz.* [7–10],

$$\frac{\partial\phi}{\partial t} = \Gamma_\phi\nabla^2\frac{\delta F(\phi,\psi)}{\delta\phi}, \tag{5}$$

$$\frac{\partial\psi}{\partial t} = -\Gamma_\psi\frac{\delta F(\phi,\psi)}{\delta\psi}, \tag{6}$$

where $\delta/\delta\psi$ and $\delta/\delta\phi$ are the functional derivatives with respective to the crystal order parameter or concentration. Γ_ψ is the mobility representing the propagation of the crystal-melt interface, which is inversely proportional to the viscosity or the frictional coefficient, whereas Γ_ϕ is the analogous mobility pertaining to the compositional order parameter. Equation (5) was originally introduced by Cahn and Hilliard [9] (hereafter called the Cahn-Hilliard time evolution equation), which is also known as TDGL model B. In view of the inherent anisotropy of chain molecules, polymer crystallization is expected to be anisotropic; therefore, the coefficients of the order parameters should be treated in a tensorial form to capture the directional growth. However, polymer spherulites are more or less symmetric, and thus the crystal order parameter and its coefficients may be treated in a scalar form,

$$\frac{\partial\phi}{\partial t} = \Gamma_\phi\nabla^2[(\phi+\phi^3) - \kappa_\phi\nabla^2\phi - \psi(\alpha_1 + \alpha_2\psi + 2\alpha_3\phi)], \tag{7}$$

$$\frac{\partial\psi}{\partial t} = -\Gamma_\psi[W_\psi\psi(\psi-\zeta)(\psi-\psi_0) - \kappa_\psi\nabla^2\psi - \phi(\alpha_1 + 2\alpha_2\psi + \alpha_3\phi)]. \tag{8}$$

The interface gradient coefficient, κ_ϕ, may be treated simply as constant. As pointed out above, the asymmetric double well of the ψ order parameter in Fig. 1 represents the local free energy density that explains how phase transition occurs from the melt ($\phi=0$) to the solid crystal ($\psi<1$ for a given supercooling or $\psi=1$ only at equilibrium). The addition of the coupling terms in Eq. (4) indeed exerts profound effects on thermodynamics and kinetics, especially the time-evolution equations (7) and (8): (i) The linear coupling term allows the two fields to copy each other. (ii) The quadratic dependence of ψ in the second coupling term has no influence on the shape (or position of the minimum) of the double well in ψ, but the magnitude of the height of the unstable hump can change slightly. Hence the coefficient α_2 is set to zero in all of our calculations. (iii) On the other hand, the quadratic dependence of ϕ in the third coupling term, affects the crystallization habit directly, i.e., it affects the nucleation rate. Given $\alpha_1=1$, as ϕ is positive, it becomes easier for the

occurrence of nucleation since the height of nucleation barrier is getting smaller and its location shift to lower value on the ψ axis, and thus the local position is occupied by the crystals; on the contrary, when ϕ is negative, it is more difficult for the nucleation to occur, consequently, the local region is filled with amorphous materials. In other words, this kind of influence on nucleation rate depends on the sign and the amount of ϕ.

In the calculation of the time evolution of the compositional order parameter (ϕ) of Eq. (7), the values of the expansion coefficients, r and u, are taken as unity having the same sign for a single well potential and α_2 and α_3 may be set as zero for the simplest linear coupling case, leaving the linear coupling term only. More importantly, these model parameters in Eq. (8) can be expressed in terms of the material parameters (most of which can be determined experimentally) [1,2,12] such as heat of fusion, ΔH_u, supercooling, $\Delta T = T_m^0 - T$. Thus, these model parameters can be evaluated according to the following relations:

$$\psi^* = \frac{T_m^0 - T_m}{T_m^0 - T}, \quad \xi = \frac{4\psi_0\psi^* - 3\psi^{*2}}{6\psi_0 - 4\psi^*}, \tag{9}$$

$$W_\psi = 6\frac{\Delta H_u}{nRT}\left(\frac{T_m - T}{T_m^0}\right)\left(\frac{\psi_0}{2} - \xi\right)^{-1}, \tag{10}$$

$$\kappa_\psi = 72\left(\frac{\sigma}{nRT}\right)^2 \frac{1}{W_\psi}, \tag{11}$$

$$\Gamma = \frac{\sqrt{2}}{12} v \left[\frac{\sigma}{nRT}\left(\frac{\psi_0}{2} - \zeta\right)\right]^{-1}, \tag{12}$$

where ΔH_u is the heat of fusion of the crystal, n is the molar density, σ is the solid-liquid interface energy, and v is the velocity of the interface. ψ^* is a critical order parameter (ψ), which is related to the supercooling or the domain size. It should be emphasized that the model parameters, Γ_ψ, κ_ψ, W_ψ, and ζ can essentially be estimated from the experiment [1,13–16]. As evidenced in Eqs. (9)–(12), all these model parameters are dependent on supercooling. Hence, a small change in experimental crystallization temperature could alter the values of the above model parameters significantly, thereby the emerging morphology drastically.

Physically, $\psi=0$ corresponds to the melt state, whereas $\psi=\psi_0$ represents the metastable solid crystal that is a function of supercooling according to the Hoffman-Weeks relationship [15]. At equilibrium, $T=T_m^0$ (i.e., $\zeta=1/2$), the local free energy minima of the crystal and melt states are equivalent (Fig. 1). When $T>T_m^0$, the free energy density of the crystal is higher than that of the melt, so the crystal must melt. On the other hand, when $T<T_m^0$, the global minimum is located at the crystalline state, so the metastable melt undergoes crystallization by overcoming the nucleation barrier. From Eq. (9), it is evident that the parameter ζ (T) depends on the supercooling, i.e., the smaller the ξ value, the larger the supercooling. Usually the equation is expressed in a dimensionless form with dimensionless time τ and dimensionless variables denoted with tilde symbols as follows: $\tilde{x}=x/d^*$, $\tilde{y}=y/d^*$, $\tau=Dt/d^{*2}$, where d^* is the characteristic length scale and D the translational diffusion coefficient; then, one obtains the final governing equations, *viz.*,

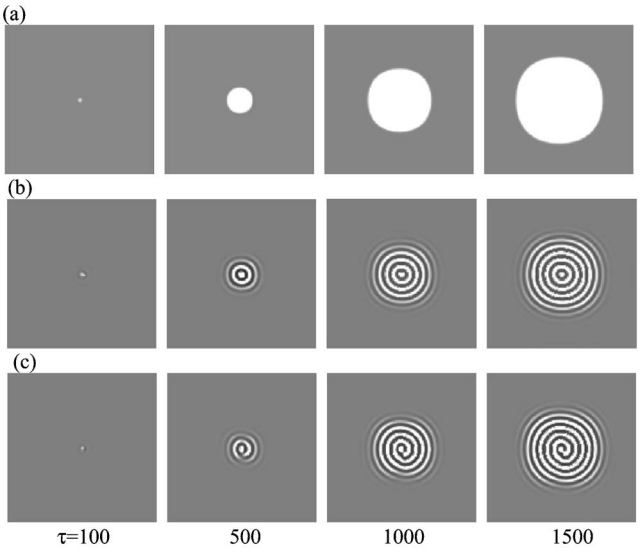

FIG. 2. Temporal evolution of the crystal order parameter (a) circular ($\alpha_1=0.001$, $\alpha_2=0$, $\alpha_3=0$; representing weak interaction), (b) target and (c) spiral patterns ($\alpha_1=0.5$, $\alpha_2=0$, $\alpha_3=0.1$; representing strong interaction) exhibiting the emergence of textureless regular, concentric ringed, and spiral spherulites in two dimensions, respectively. The model parameters: $\Gamma_\psi=10^5$, $W_\psi=0.1$, $\zeta=0.3$, $\Gamma_\phi=0.1$, and $\kappa_\phi=1$ are the same for the three cases.

$$\frac{\partial\phi}{\partial\tau} = \tilde{\Gamma}_\phi \nabla^2[(\phi + \phi^3) - \tilde{\kappa}_\phi \tilde{\nabla}^2\phi - \alpha_1\psi], \tag{13}$$

$$\frac{\partial\psi}{\partial\tau} = -\tilde{\Gamma}_\psi\{W_\psi\psi(\psi - \psi_0)[\psi - \xi(T)] - \tilde{\kappa}_\psi\tilde{\nabla}^2\psi - \alpha_1\phi\}, \tag{14}$$

where $\tilde{\nabla} = \tilde{i}(\partial/\partial\tilde{x}) + \tilde{j}(\partial/\partial\tilde{y})$, $\tilde{\Gamma}_\phi = \Gamma_\phi d^{*2}/D$, $\tilde{\kappa}_\phi = \kappa_\phi/d^{*2}$, $\tilde{\Gamma}_\psi = \Gamma_\psi d^{*2}/D$, and $\tilde{\kappa}_\psi = \kappa_\psi/d^{*2}$. Note that Eqs. (13) and (14) represent the simplest linear coupling case for demonstration purposes.

It should be emphasized that the two propagating waves represented by Eqs. (7) and (8) individually have kink-type solitary wave solutions [11]. However, when these waves collide and interfere mutually during crystallization, the resultant wave, under certain conditions, can transform from the kink-type solitary to the oscillatory wave [17,18]. Such wave collisions, in turn, generate a rich variety of morphologies [19–21]. The formation of various morphological patterns may be demonstrated by simply varying the strength of the coupling coefficients, keeping the same model parameters: $\Gamma_\psi=0.1$, $W_\psi=1$, $\kappa_\psi=0.1$, $\zeta=0.3$, and $\Gamma_\phi=0.1$ for the following three cases. With a weak coupling coefficient ($\alpha_1=0.001$, $\alpha_2=0$, $\alpha_3=0$), a circular pattern (in two dimensions) emerges, which is the manifestation of the solitary kink wave in the one-dimensional slice [Fig. 2(a)]. With increasing strength of the coupling coefficient ($\alpha_1=0.5$, $\alpha_2=0$, $\alpha_3=0.1$), the interference of the two waves becomes stronger, which eventually drives the system to become unstable and undergo

oscillatory motion, thereby showing a concentric ringed pattern [Fig. 2(b)]. Under more or less the same conditions as those of the target pattern, a spiral pattern occasionally develops, which seemingly depends on the random number generation in triggering the nuclei [Fig. 2(c)]. It should be emphasized that these spirals are probably random occurrence; nevertheless, such event indeed occurs in nature frequently. These concentric rings and spiral growth patterns are stable as opposed to the pulsating target patterns in the excitable media.

EXPERIMENTAL SECTION

Poly(vinylidene) fluoride (PVDF), supplied kindly by Kureha Chemical Industry, has weight-average molecular weight $M_w = 246\,000$ and number average molecular weight $M_n = 144\,000$. Poly(ethylene-co-vinyl acetate) (EVAc-80) (the number indicates wt % EVAc) was purchased from Dai Nippon Ink & Chemicals, Inc. The constituent polymers were dissolved separately in the 90/10 mixed solvent containing *N*, *N'*-dimethyl acetamide and tetrahydrofuran. The polymer concentration was 5wt %. The solutions were then mixed in desired proportions. These blends were cast onto cover glasses to form thin films (10 μm thick) through evaporation of solvent at ambient temperature. The cast films were further dried under vacuum for 1 week at room temperature. To ensure the complete solvent removal, these film specimens were melted at 200 °C in a hot plate for 10 min prior to each experiment.

The structural evolution of PVDF spherulites was monitored using Nikon (Optiphot 2-pol) equipped with a Nikon camera (FX-35DX) and a color charge-coupled detector (CCD) camera (SSC-DC34, Sony). The light source was a Halogen bulb operated at 100 W and 12 V. Solvent cast samples were used for microscope observations. The sample heating chamber (model FP82 HT, Mettler Toledo) equipped with a programmable temperature controller (FP90 central processor, Mettler Toledo) was used to control the temperature. The film exposure time was automatically controlled depending on the intensity of transmitted light. Temperature quench experiments were undertaken in an optical microscope hot stage by rapidly transferring the blend specimen from 200 °C to various experimental temperatures. Real-time observations of the change in morphology at a given temperature were observed using the Sony CCD camera, interfaced with a personal computer. Asymmetrix digital video acquisition software was utilized to obtain a digital image.

For morphological characterization, an atomic force microscope (AFM) (Seiko Instruments SPI 3,600), equipped with a Si_3N_4-type cantilever, was utilized. The AFM consisted of a small probe mounted in a scanner, a stage supporting the scanner, an electronic interface unit (EIU), and a computer. A tapping mode was used to characterize the phase contrast between the emerged crystal region and the noncrystalline materials at room temperature.

RESULTS AND DISCUSSION

Figure 3 depicts the optical micrographs exhibiting the time sequence of the spiral spherulites of PVDF in the blends

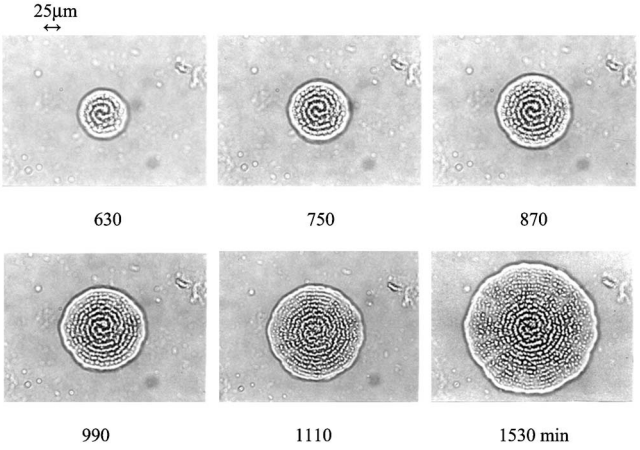

FIG. 3. Optical micrographs showing the time sequence of the evolution of spiral spherulite undergoing breakup of the spiral arms in the blend of 90/10 PVDF/EVA-80 during isothermal crystallization at 170 °C.

of 90/10 PVDF/EVA-80 subjected to isothermal crystallization at 170 °C. It is evident that a two-arm spiral developed at the core with a sense in the counterclockwise direction (630 min). In some cases [1], a single-arm spiral emerges. As the probability of having a sense of rotation in the clockwise or counterclockwise is the same, it is not surprising to occasionally discern spirals with clockwise and/or counterclockwise rotations under the same microscopic view [1,2]. As the spiral tips propagate, the arms are seemingly fragmented due to the growth instability caused presumably by rejection of EVA chains as well as of amorphous PVDF molecules not only into the interspiral region but also into the intraspiral region (i.e., the interlamellar region), thereby causing the spiral to eventually break up into lamellar aggregates. The fragmented lamellar aggregate morphology becomes more distinct as the spherulite continues to grow. It is noticed that the spiral breakup occurs only when the crystallization temperature is very close to the melting temperature of the PVDF crystals in the blends, i.e., very shallow supercooling.

In principle, the exothermic heat generated during crystallization could locally melt the existing crystals, which in turn crystallize again. Such a melting-recrystallization process is expected to occur at the crystallizing fronts; hence, it could lead to the breakup of the spiral tips. However, this mechanism cannot explain as to why the spiral breakup has to occur in a regular periodic manner. It should be noted that the present intriguing observation of the spiral breakup reveals striking similarity to those of the dissipative systems and excitable media, and thus the unusual spiral breakup phenomenon in polymer crystallization deserves close scrutiny.

Now, the challenge is whether the proposed phase field model can capture the breakup of spiral and concentric ringed spherulites. The numerical simulation was undertaken on a square lattice 1024×1024 based on an explicit method for the temporal steps and a finite difference scheme for the spatial steps with no flux boundary conditions. Various grid sizes and temporal steps have been employed to ensure the

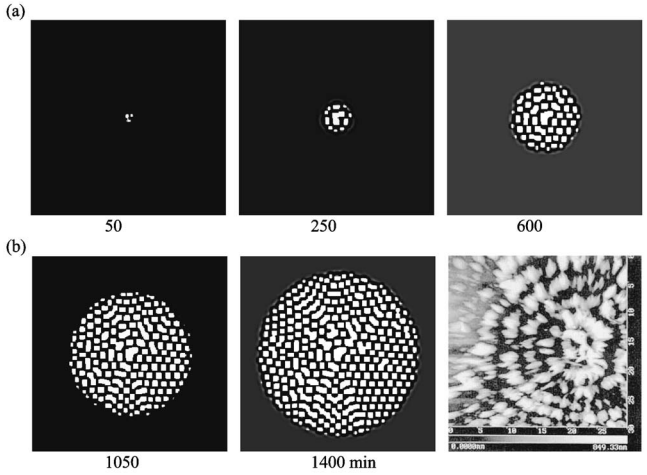

FIG. 4. (a) Time evolution of the crystal order parameter showing a broken spiral spherulite in miscible blends calculated based on the parameters $\Gamma_\phi=0.1$, $\kappa_\phi=1$, $\zeta=0.3$ (170 °C), and $\alpha_1=1$, representing strong coupling, in comparison with (b) atomic force micrograph (phase mode) of the 90/10 PVDF/EVA-80 blends crystallized at 170 °C. All model parameters pertaining to the crystal phase field order parameter utilized were evaluated from the known materials parameters and the experimental conditions as listed in Table I.

stability of the simulation. In view of the high penalty of creating an interface, nuclei of the lower free energy phase (i.e., crystals) can be grown only when thermal fluctuations are sufficiently large. To avoid overcrowding of the nuclei, a single thermal perturbation is imparted in triggering a nucleation event, which is the basis for interfacial genesis. Once an interface is formed, the crystal grows in a manner that is controlled by the interface diffusion and the local free energy difference across the interface. In the simulation, d^* and D are taken as 1×10^{-7} m and 1×10^{-15} m^2 s^{-1}, respectively.

Figure 4 exhibits the temporal evolution of the fragmented spiral/concentric ringed spherulite calculated for a given supercooling ($\zeta=0.3$) in comparison to that of the phase contrast atomic force micrograph (AFM) (model SPI 3,600, Seiko Instruments) of the 90/10 PVDF/EVA-80 blend crystallized at 170 °C. Taking T_m^0 to be 189 °C [16], the value of ζ (i.e., $\zeta=0.3$) corresponds to 170 °C (Table I). The emerged initial nucleus is of irregular shape, but it evolves seemingly into a spiral pattern. Except for an early stage, the broken spiral spherulite is indistinguishable from that of the concentric ringed spherulite. As evidenced in the phase-mode AFM picture, the spiral rings are fragmented into the lamellar aggregates. It is also noticed that the spacing between the broken spiral rings appears regular. Strikingly, the present calculation captures the periodic breakup of the spiral pattern, which is exactly what was seen in the AFM picture. It may be hypothesized that since the crystallization of PVDF in the blends with PVAc as well as with EVA is rhythmic and exhibits periodic target and/or spiral patterns, the spherulitic growth could be periodic not only in the interspirals (spacing between the neighboring spiral arms/rings) but also in the intraspiral direction.

Figure 5 shows the emerged spiral spherulites at various ζ values ranging from 0.1 to 0.4 corresponding to very deep and very shallow supercoolings, respectively. When the isothermal crystallization temperature is very close to the equilibrium melting, i.e., $\zeta=0.4$, the nucleus cannot grow effectively. On the other hand, when the supercooling is very large, say $\zeta=0.1$, a regular spiral spherulite develops in both compositional and orientational order parameter fields. At intermediate ζ values, the spiral arms become increasingly unstable with increasing isothermal crystallization temperature. The spiral arm at the core is fragmented initially, but the broken spiral arm is reconnected again in time (picture not shown) and further evolves into the spiral spherulite with dislocated faults running radially outward from the common center (see the picture at $\zeta=0.2$). At $\zeta=0.3$, the spirals are broken into smaller pieces; and the fragmented spiral pattern becomes practically indistinguishable from that of the concentric rings. The great similarity between the calculated fragmented spirals and the observed lamellar aggregates in the fragmented spherulite suggests that the major controlling factor for the breakup of spirals and/or concentric rings in polymer spherulites during isothermal crystallization is undoubtedly the supercooling. It is reasonable to conclude that the supercooling not only influence the domain size (e.g., the periodic length scale of the spiral and concentric rings) but also alters the types of spherulitic morphologies formed.

TABLE I. Model simulation parameters calculated in accordance with Eqs. (9)–(12) using the material and physical parameters of PVDF for a particular case of $\zeta=0.3$ at 170 °C. Note that all these simulation parameters are supercooling dependent, and thus their values would change depending on the experimental temperature for crystallization.

Material parameters	Model parameters
$\Delta H_u=60$ J/g[a]	$\Gamma_\psi=10^5$ s^{-1}
$T_m^0=189$ °C	$W_\psi=1.76$
$T_m=180$ °C	$\kappa_\psi=3.86\times10^{-18}$ m^2
$T_c=170$ °C	$\psi_0=0.95$
$\sigma=0.0332$ J/m^{2}[b]	$\zeta=0.3$

[a]Reference [13].
[b]Reference [14].

The question arises as to why the spherulitic patterns in the ψ and ϕ order parameter fields appear identical. As can be envisaged in Eqs. (4), (7), and (8) that the first linear coupling term allows the two order parameter ψ and ϕ fields to copy each other during each iteration, therefore these images appear the same. If one used a large coefficient of α_3 (quadratic dependence of ψ) to α_1, then the two images would appear differently. In the actual experiment, the spherulitic morphologies show similar appearance for both the cross polarizers (that mimic the orientation fluctuation or crystal order parameter) and without polarizers (i.e., refractive index differences showing the concentration fluctuation). Hence, we put a greater weight on the α_1 relative to α_3 in Eq. (4) that gives more realistic patterns similar to our actual experimental observation [1].

There is no doubt that the liquid-liquid phase separation between amorphous PVDF and EVAc-80 chains would further complicate the morphology forming process. However,

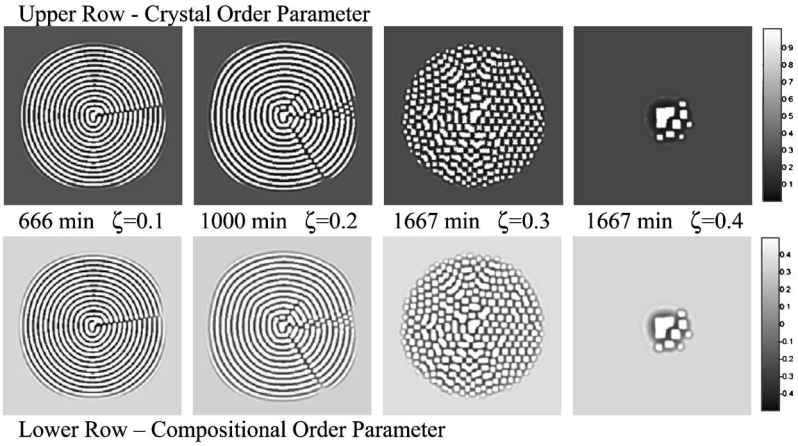

FIG. 5. Effect of ζ on the emerged spiral spherulite, signifying the effect of supercooling on morphology development in miscible blends. The parameters used in the simulation were $\Gamma_\phi=0.1$, $\kappa_\phi=1$, and $\alpha_1=1$. ($\zeta=0.1$, 0.2, 0.3, and 0.4 corresponds to the crystallization temperature of 135 °C, 160 °C, 170 °C, and 176 °C respectively.) The crystal order parameter ranges from $(0\leqslant\psi\leqslant1)$ with a scale color bar represented by black at $\psi=0$ and white color at $\psi=1$. The compositional order parameter was carried out in the range of $(-0.5\leqslant\phi\leqslant0.5)$ with a scale bar represented by black at $\phi=-0.5$, white at $\phi=0.5$, and the average gray at $\phi=0$, and the background is approximately $\phi=0.4$, corresponding to the average concentration of the 90/10 PVDF/EVA blend.

the present system is miscible in the amorphous state, and thus the effect of phase separation on the emerging crystalline morphology was not explored. Moreover, the mechanism of the lamellar twisting was not built in the model as yet because one needs to redefine the present scalar crystal order parameter in a vector form and also the simulation must be carried out in three dimensions in order to capture the twist, which is reserved for the scope of a future work.

CONCLUSIONS

In summary, we have demonstrated that the phase field model of solidification based on the TDGL model C is capable of capturing the breakup of spiral spherulites during isothermal crystallization. It is reasonable to conclude that the phenomenon of spiral breakup in polymer spherulites is governed predominantly by the supercooling. This observation is not surprising in view of the fact that the model parameters depend directly or indirectly on the supercooling [see Eqs. (9)–(12)] therefore a slight change in the experimental crystallization temperature or the supercooling could alter the model parameters profoundly, and hence the emerging structure. It should be emphasized that the supercooling not only affects the domain size (e.g., the periodic length scale of the spiral arms and concentric rings), but also exerts profound influence on the types of spherulitic morphologies formed.

ACKNOWLEDGMENTS

The present study is made possible by the support of National Science Foundation through the Grant No. DMR 02-09272, and the Ohio Board of Regents through a Research Challenge Grant. Y.O. is indebted to Sumitomo Electrics Industries, Ltd. for financial support during his sabbatical leave at the University of Akron.

[1] Y. Okabe, T. Kyu, H. Saito, and T. Inoue, Macromolecules **31**, 5823 (1998).
[2] T. Kyu, H.-W. Chiu, A. J. Guenthner, Y. Okabe, H. Saito, and T. Inoue, Phys. Rev. Lett. **83**, 2749 (1999).
[3] *Nonlinear Wave Processes in Excitable Media*, edited by A. V. Holden, M. Marcus, and H. G. Othmer (Plenum Press, New York, 1991).
[4] J. S. Langer, in *Directions in Condensed Matter*, edited by G. Grinstein and G. Mazenko (World Scientific, Singapore, 1986), p. 164.
[5] A. A. Wheeler, W. J. Boettinger, and G. B. McFadden, Phys. Rev. A **45**, 7424 (1992).
[6] R. Kobayashi, Physica D **63**, 410 (1993).
[7] B. I. Halperin, P. C. Hohenberg, and S. K. Ma, Phys. Rev. B **10**, 139 (1974).
[8] J. D. Gunton, M. San Miguel, P. S. Sahni, in *Phase Transitions and Critical Phenomena*, edited by C. Domb and J. L. Lebowitz (Academic Press, New York, 1983), p. 267.
[9] J. W. Cahn and J. E. Hilliard, J. Chem. Phys. **28**, 258 (1958).
[10] S. M. Allen and J. W. Cahn, Acta Metall. **27**, 1085 (1979).
[11] T. Kyu, R. Mehta, and H.-W. Chiu, Phys. Rev. E **61**, 4161 (2000).
[12] F. C. Frank, J. Cryst. Growth **22**, 233 (1974).
[13] W. T. Mead, A. E. Zachariades, T. Shimada, and R. S. Porter, Macromolecules **12**, 473 (1979).
[14] S. Wu, *Polymer Interface and Adhesion* (Marcel Dekker, New York, 1982).
[15] J. D. Hoffman, and J. J. Weeks, J. Res. Natl. Bur. Stand., Sect.

A **66**, 138 (1962).
[16] J. Brandrup and E. H. Immergut, *Polymer Handbook*, 2nd ed. (Wiley Interscience, New York, 1975).
[17] K. R. Elder, F. Drolet, J. M. Kosterlitz, and M. Grant, Phys. Rev. Lett. **72**, 677 (1994).
[18] L. Granasy, T. Pusztai, G. Tegze, J. A. Warren, and J. F. Douglas, Phys. Rev. E **72**, 011605 (2005).
[19] R. Mehta, W. Keawwattana, A. L. Guenthner, and T. Kyu, Phys. Rev. E **69**, 061802 (2004).
[20] H. Xu, R. Matkar, and T. Kyu, Phys. Rev. E **72**, 011804 (2005).
[21] H. Xu, W. Keawwattana, and T. Kyu, J. Chem. Phys. **123**, 124908 (2005).